

## Methane Sources and Migration Mechanisms in Shallow Groundwaters in Parker and Hood Counties, Texas—A Heavy Noble Gas Analysis

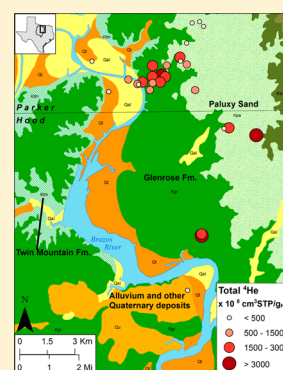
Tao Wen,<sup>†</sup> M. Clara Castro,<sup>\*,†</sup> Jean-Philippe Nicot,<sup>‡</sup> Chris M. Hall,<sup>†</sup> Toti Larson,<sup>‡</sup> Patrick Mickler,<sup>‡</sup> and Roxana Darvari<sup>‡</sup>

<sup>†</sup>University of Michigan, Department of Earth and Environmental Sciences, Ann Arbor, Michigan 48109-1005, United States

<sup>‡</sup>University of Texas at Austin, Bureau of Economic Geology, Austin, Texas 78713-8924, United States

### S Supporting Information

**ABSTRACT:** This study places constraints on the source and transport mechanisms of methane found in groundwater within the Barnett Shale footprint in Texas using dissolved noble gases, with particular emphasis on <sup>84</sup>Kr and <sup>132</sup>Xe. Dissolved methane concentrations are positively correlated with crustal <sup>4</sup>He, <sup>21</sup>Ne, and <sup>40</sup>Ar and suggest that noble gases and methane originate from common sedimentary strata, likely the Strawn Group. In contrast to most samples, four water wells with the highest dissolved methane concentrations unequivocally show strong depletion of all atmospheric noble gases (<sup>20</sup>Ne, <sup>36</sup>Ar, <sup>84</sup>Kr, <sup>132</sup>Xe) with respect to air-saturated water (ASW). This is consistent with predicted noble gas concentrations in a water phase in contact with a gas phase with initial ASW composition at 18 °C–25 °C and it suggests an in situ, highly localized gas source. All of these four water wells tap into the Strawn Group and it is likely that small gas accumulations known to be present in the shallow subsurface were reached. Additionally, lack of correlation of <sup>84</sup>Kr/<sup>36</sup>Ar and <sup>132</sup>Xe/<sup>36</sup>Ar fractionation levels along with <sup>4</sup>He/<sup>20</sup>Ne with distance to the nearest gas production wells does not support the notion that methane present in these groundwaters migrated from nearby production wells either conventional or using hydraulic fracturing techniques.



## INTRODUCTION

With rising demands for domestic energy resources, unconventional hydrocarbon production has been extensively developed since the early 2000s.<sup>1</sup> The combined use of hydraulic fracturing (HF) and horizontal drilling has greatly increased the hydrocarbon recovery from shales, tight formations and other unconventional reservoirs.<sup>1,2</sup> As a result, unconventional gas resources (e.g., so-called shale gas) accounted for more than one-third of the total natural gas production in the United States in 2013.<sup>1,3</sup> However, the occasional presence of elevated concentrations of light hydrocarbons in nearby shallow drinking groundwater has caused public concern. For example, enhanced permeability in targeted formations such as the Marcellus or Barnett Shales (at depths of 1800 m to >2000 m) may facilitate migration of natural gas, formation brines and other contaminants into shallow aquifers (<500 m), thereby threatening drinking-water supplies.<sup>2,4–7</sup> Previous work has focused on identifying sources of methane in shallow groundwaters, for example, the Trinity Aquifer in the Barnett Shale footprint, which can be either from thermogenic or microbial sources.<sup>4–6,8–11</sup> It should be noted, however, that the occurrence of both thermogenic and microbial gas in shallow groundwater could be due to either natural or anthropogenic causes.<sup>8,9,12,13</sup>

The Barnett Shale in the Fort Worth Basin is the oldest shale gas play in which HF became a major stimulation technique.<sup>1</sup>

Large sections of the basin have also undergone conventional production for decades, including the study area where most of the produced gas originated from the Strawn Group. Within the Barnett Shale footprint, the presence of localized stray gas in the shallow Trinity Aquifer has been investigated with respect to its migration mechanisms and origin in several studies.<sup>8,9</sup> Here, “stray gas” refers to natural gas present in shallow aquifers of an undetermined origin. In addition, the descriptor “Trinity Aquifer” is understood as water-bearing rocks mostly of the Trinity Group of Cretaceous age but that can also include the occasional sandstones of the Paleozoic Strawn Group in hydrogeologic continuity with them. Based on well headspace observations of hydrocarbon molar ( $[\text{C}_2\text{H}_6^+]/[\text{CH}_4]$ ), stable isotopic (e.g.,  $\delta^{13}\text{C}-\text{CH}_4$ ) ratios and other information, Kornacki and McCaffrey<sup>9</sup> tentatively concluded that stray gas in shallow water wells in the Trinity Aquifer within Parker county is of thermogenic origin and originates from the Strawn Group as opposed to the deep Barnett Shale. However, microbial activity and oxidation can alter the original geochemical signature and thus, obscure the original sources and/or mechanisms of fluid migration.<sup>5,8,14</sup>

Received: March 25, 2016

Revised: September 6, 2016

Accepted: September 29, 2016

Published: September 29, 2016

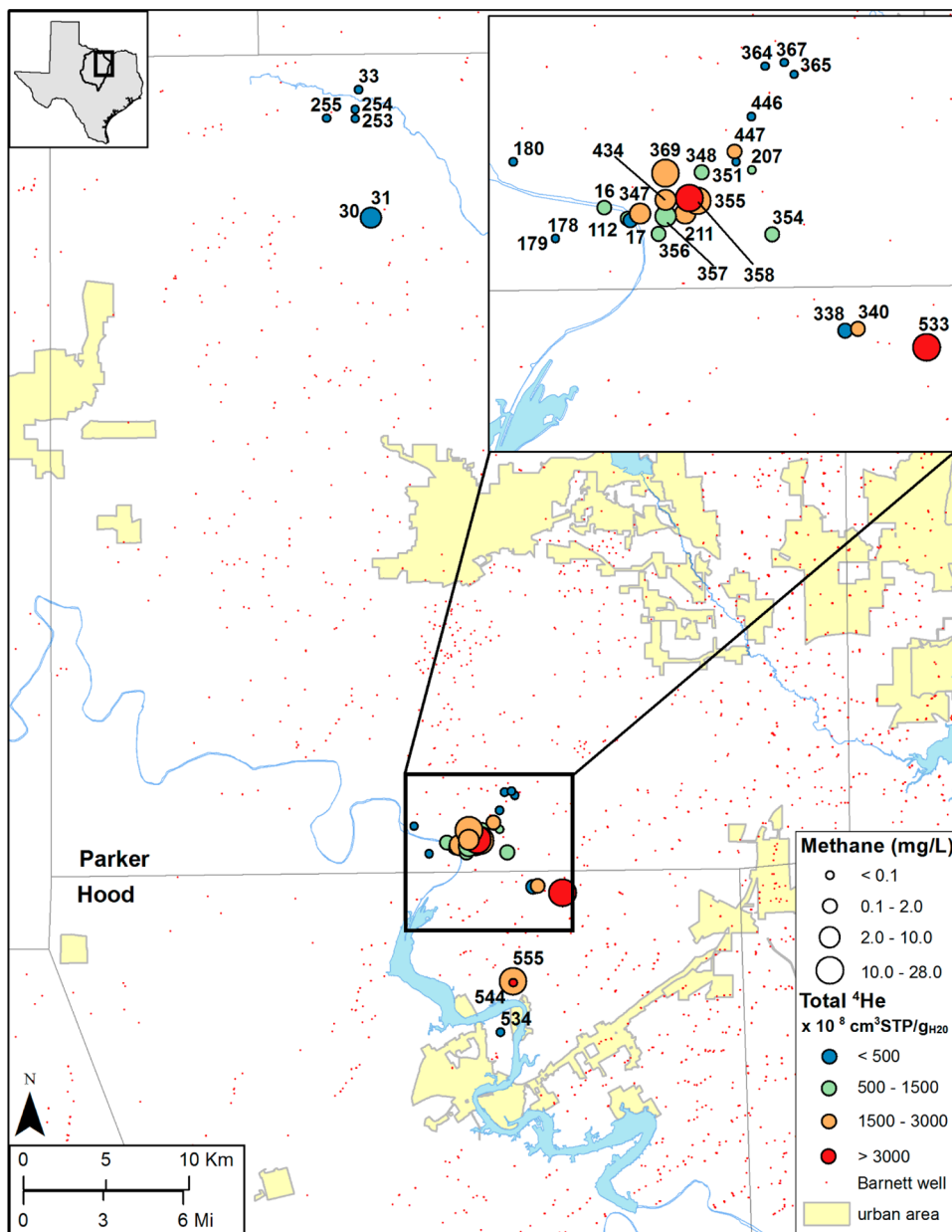


**Figure 1.** Spatial distribution maps of dissolved methane and total <sup>4</sup>He concentrations for sampled Trinity Aquifer wells. The South Cluster is located close to the Brazos River between the City of Granbury to the south and the City of Weatherford to the north whereas the North Cluster is located north of the City of Weatherford. Small red dots represent wellhead locations of horizontal wells producing from the Barnett Shale.

In contrast, stable noble gases (Helium – He, Neon – Ne, Argon – Ar, Krypton – Kr, Xenon - Xe) are chemically inert and are thus transported without being affected by chemical reactions.<sup>15,16</sup> Noble gases in subsurface fluids (e.g., freshwater, natural gas) are derived from the atmosphere, crust, and mantle, all of which show distinct isotopic and elemental signatures.<sup>15–19</sup> This makes noble gases ideal natural tracers for studying the origin and evolution of crustal fluids in sedimentary basins.<sup>16,20–29</sup> In most subsurface fluids in sedimentary systems, noble gases are dominated by an atmospheric origin (air saturated water or ASW) and/or a crustal component deriving primarily from radioactive decay of U, Th and <sup>40</sup>K.<sup>15</sup> In this study, the crustal component is identified with the “\*” notation.

Previous noble gas work on natural gas from the Barnett and Strawn formations and from the shallow Trinity Aquifer in the

Barnett Shale footprint in Parker county suggested that dissolved methane in groundwater is likely derived from the Strawn Group.<sup>8</sup> Some of this stray gas would presumably have migrated along the annulus of a producing well due to poor cementation.<sup>8</sup>

Here, we present noble gas concentrations and isotopic ratios from groundwater samples collected in the Trinity Aquifer within the Barnett Shale footprint in Parker and Hood counties in north-central Texas (Figure 1). This data, together with information provided by well logs of the sampled water wells is used in an attempt to clarify both the origin of stray gas in the Trinity Aquifer, as well as potential mechanisms responsible for its migration from its source into the Trinity Aquifer water wells. Based on collected data, at this stage, our findings do not point specifically to anthropogenic causes (e.g., poor-quality cementing of natural gas production wells either conventional

or using HF technology) that would be responsible for the presence of methane in the Trinity Aquifer in Parker County.

## MATERIALS AND METHODS

**Barnett Shale, Strawn Group, and Trinity Aquifer.** The Fort Worth Basin, where the Barnett Shale and Strawn Group are located, is a north–south elongated trough covering roughly 38 100 km<sup>2</sup> in north-central Texas in the southern United States (Figure S1; Supporting Information (SI)).<sup>1,30</sup> It is floored by a Precambrian basement. The Barnett Shale of Late Mississippian age (~331–323 Ma) is the primary petroleum source rock in the Fort Worth Basin and found at a depth of ~1800 m in the study area (SI Figure S2).<sup>2,30–34</sup> Overlying the Barnett Shale are, from oldest to youngest, the ~150–200 m thick Marble Falls (mostly carbonates) and ~600–700 m thick mostly siliciclastic Bend/Atoka Formations, of Late Mississippian and Lower Pennsylvanian age (~323–299 Ma).<sup>3,35,36</sup> The 650–750 m thick Lower Strawn (Kickapoo Creek Formation) unconformably overlain by Cretaceous rocks in the study area consists of alternating sandstone and dominant shale layers with episodic carbonates.<sup>36</sup> Both the Strawn Group and the overlying Cretaceous formations include also minor coal seams.<sup>9,37,38</sup> Montgomery et al.<sup>31</sup> and Pollastro et al.<sup>30</sup> suggested that significant migration of hydrocarbons occurred from the Barnett Shale into the Strawn Group over geologic times charging commercially produced reservoirs. The timing of migration, however, is poorly constrained.

The Trinity Group hosting the Trinity Aquifer is the main source of drinking water in Parker and Hood counties, where it crops out.<sup>8,9,39</sup> The Trinity Aquifer locally consists of sandstones, silts and conglomerates overlaid by the carbonate Glenrose Formation that acts as a confining unit. In the study area, the Cretaceous sedimentary cover is very thin (<200 m; cf. SI Text S1). Basal sands of the Trinity Group overlie the Strawn Group in an angular unconformity (SI Figure S2).<sup>9,40</sup> Predevelopment hydraulic heads in the Trinity Aquifer indicate that the general direction of flow in the study area is along dip from the outcrop to the East.<sup>40</sup>

There are no mapped faults at the surface in Parker and Hood counties but several exist at depth, impacting at least some of the Paleozoic section. In addition to the Ouachita thrust belt on the eastern edge of the Barnett, a major fault, “the Mineral Wells fault”, trending SW-NE is present in southern Denton and northern Parker counties (SI Figure S1).<sup>30,41</sup> This fault, which was active throughout the Paleozoic, appears to be rooted in the Precambrian basement.<sup>30,31</sup> Several minor normal faults parallel to it are present in the Fort Worth Basin, including in southern Parker county.<sup>30</sup>

**Sampling and Analytical Methods.** Forty-five groundwater samples were collected from 35 wells for measurement of He, Ne, Ar, Kr, and Xe concentrations and their respective isotopic ratios (Table S1; Figure 1; Supporting Information). Duplicates were collected from 10 well sites (SI Table S1). Groundwater samples were collected in standard refrigeration grade <sup>3/8</sup>” Cu tubing after temperature, pH and electrical conductivity reached equilibrium. Cu tubes were sealed by steel pinch-off clamps<sup>42</sup> after water was allowed to flush through the system for approximately 10 min.

The complete measurement procedure for groundwater samples was carried out in the Noble Gas Laboratory at the University of Michigan. Additional sampling, extraction and purification procedures can be found in the literature.<sup>17,28</sup> He and Ne were analyzed in a Thermo Scientific Helix SFT mass

spectrometer while Ar, Kr, and Xe were sequentially inlet into an ARGUS VI mass spectrometer using a computer-controlled double-head cryo-separator. Analysis procedures are described in the SI Text S2.

Groundwater samples were also collected in glass serum vials with thick rubber septa for CH<sub>4</sub> concentrations following Kampbell and Vandegrift<sup>43</sup> as described in Nicot et al.<sup>35</sup> and were analyzed at The University of Texas at Austin (UT).<sup>35</sup> The detection limit was 0.001 mg/L for dissolved methane.<sup>43</sup> It should be noted, however, that this sampling approach could underestimate oversaturated CH<sub>4</sub> concentrations in water. Collected water samples for Cl<sup>-</sup> concentrations (SI Table S5) were also analyzed at the UT Bureau of Economic Geology (BEG).<sup>35</sup>

## RESULTS AND DISCUSSION

**Spatial Distribution of Dissolved Methane.** Groundwater samples in the Trinity Aquifer are grouped into two clusters based on their location (Figure 1; SI Table S1): (1) the “south cluster”, for samples located in Hood and Parker counties, proximal to the boundary between the counties, where high dissolved methane concentrations were previously documented,<sup>8,9</sup> and; (2) the “north cluster”, for samples located in the northern portion of Parker county, that was chosen to be away from the south cluster where high methane concentrations are known to be present. With the exception of one sample (i.e., sample 31) noted in the discussion, all the dissolved methane carries the signature of a thermogenic origin, relatively heavy  $\delta^{13}\text{C}$  (–54.1‰ to –26.2‰) and is accompanied by ethane and propane.<sup>35</sup>

Following the classification of methane concentrations dissolved in groundwater by Eltschlager et al.,<sup>44</sup> only five groundwater samples all from the “south cluster” (samples 355, 358, 369, 533, and 555) display dissolved methane concentrations of concern, that is, >10 mg/L (SI Table S1). In addition, five samples show methane concentrations between 2 and 10 mg/L, whereas 25 out of 35 wells display dissolved methane concentrations of 0.1–2 mg/L. Many of these wells are located in the proximity of natural gas wells currently being exploited both in the Barnett (using HF techniques) and the Strawn (conventional exploitation) formations, but no strong and definite spatial correlation has been observed between these production wells and water wells displaying high dissolved methane concentrations.<sup>35</sup> In addition, water wells with concentrations >2 mg/L are located in close proximity to wells with low and trace methane concentrations (Figure 1). These spatial observations suggest, a priori, a lack of correlation between high dissolved methane concentrations and the locations of natural gas production wells from either the Barnett Shale or the Strawn Group.

**Noble Gas Signatures versus Methane Content.** Total dissolved <sup>4</sup>He, <sup>20</sup>Ne, <sup>36</sup>Ar, <sup>84</sup>Kr and <sup>132</sup>Xe concentrations and isotopic ratios are listed in SI Tables S2 and S3, respectively. <sup>3</sup>He/<sup>4</sup>He ratios (R) are normalized to the atmospheric ratio Ra, where Ra = (1.384 ± 0.013) × 10<sup>-6</sup>.<sup>45</sup> Atmospheric concentrations and isotopic ratios are also reported for reference.

All groundwater samples, without exception, display <sup>4</sup>He concentrations in excess of ASW values, reaching over 3 orders of magnitude above that of ASW for temperatures ranging between 0 and 25 °C (Figure 1). Similar to the spatial distribution of dissolved methane concentrations, highest total <sup>4</sup>He concentrations are found in some of the south cluster wells

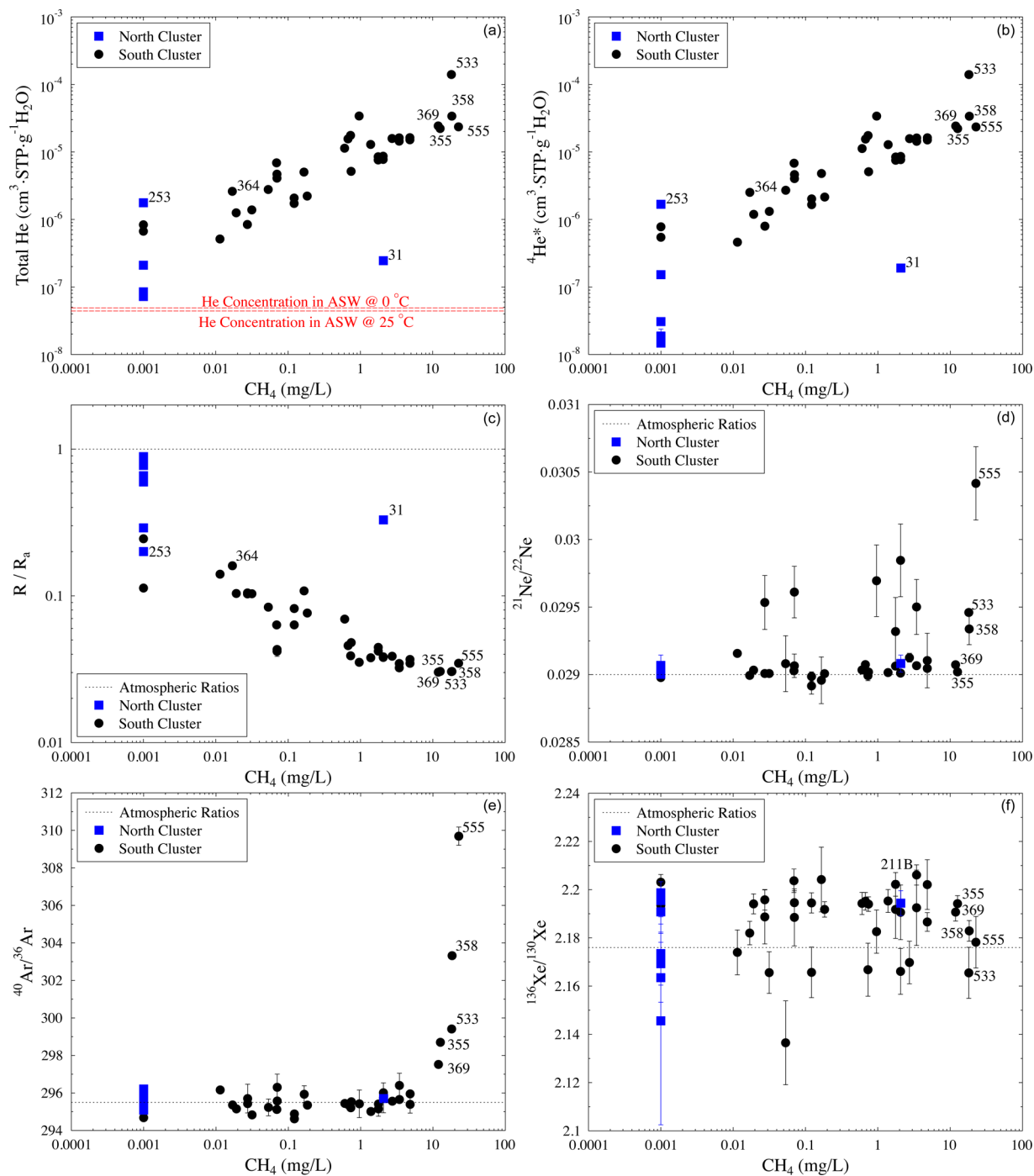


**Figure 2.** (a) Total He concentrations, (b)  $^4\text{He}^*$  concentrations, (c)  $R/R_a$  ratios, (d)  $^{21}\text{Ne}/^{22}\text{Ne}$  ratios, (e)  $^{40}\text{Ar}/^{36}\text{Ar}$  ratios, and (f)  $^{136}\text{Xe}/^{130}\text{Xe}$  as a function of measured dissolved methane concentrations in collected groundwater samples. Corresponding atmospheric noble gas values are indicated (dashed lines). Samples with undetected methane concentrations are plotted at the methane detection limit (0.001 mg/L).

(samples 355, 358, 369, 533, and 555; SI Table S2, Figure 1). Overall, a direct correlation is observed between dissolved methane and total  $^4\text{He}$  concentrations, suggesting a common source for both the stray gas and  $^4\text{He}$  present in these groundwaters (Figure 2a). Main outliers to this general trend are samples 31 and 253, both located in the north cluster. Higher methane concentrations in sample 31 are due to the presence of microbial methane (2 mg/L methane, no measured ethane,  $\delta^{13}\text{C} = -66\%$ ; cf. Nicot et al.<sup>35</sup>), whereas mantle He present in sample 253 can explain the deviation of this sample from the observed correlation between methane and total He

concentrations (Figure 2a; cf. SI Text S3). Crustal  $^4\text{He}$  concentrations ( $^4\text{He}^*$ ) are estimated following Castro and colleagues<sup>46,47</sup> and vary by over 3 orders of magnitude, from  $1.47 \times 10^{-8}$  to  $1.40 \times 10^{-4}$   $\text{cm}^3\text{STP}/\text{g}_{\text{H}_2\text{O}}$ . Similar to observations for total  $^4\text{He}$  concentrations,  $^4\text{He}^*$  concentrations display a good correlation with dissolved methane concentrations (Figure 2b). Overall, the south cluster exhibits highly contrasting dissolved methane and  $^4\text{He}^*$  concentrations within a very limited area, an observation that is consistent with previous findings.<sup>8</sup> In addition to being well correlated with dissolved methane in groundwater, concentrations of both total

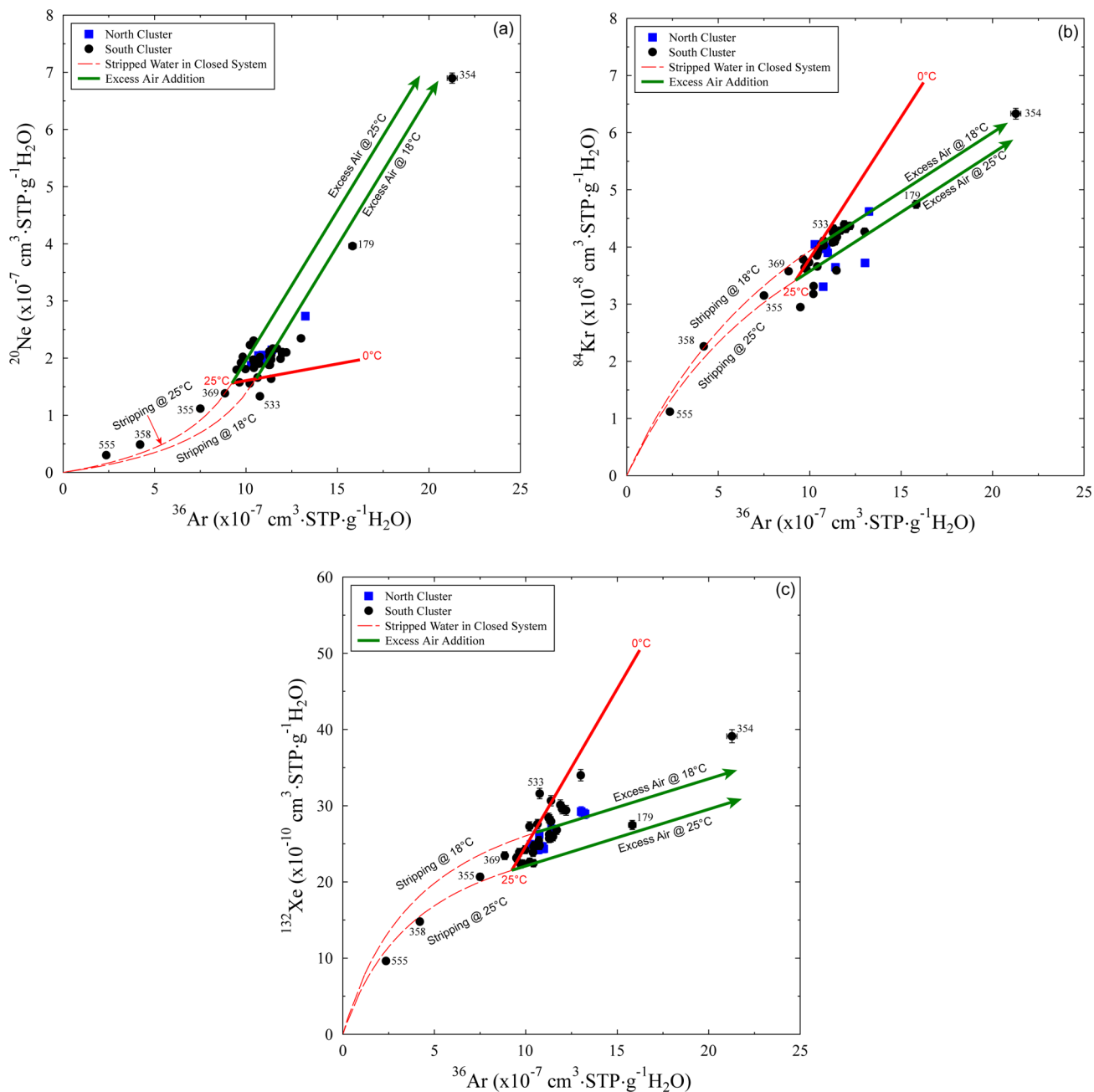


**Figure 3.** (a)  $^{20}\text{Ne}$ , (b)  $^{84}\text{Kr}$  and (c)  $^{132}\text{Xe}$  concentrations as a function of  $^{36}\text{Ar}$  concentrations for all collected Trinity groundwater samples. Predicted  $^{20}\text{Ne}$ ,  $^{36}\text{Ar}$ ,  $^{84}\text{Kr}$  and  $^{132}\text{Xe}$  concentrations in air saturated water (ASW) are shown for temperatures varying from 0 to 25 °C (red solid line). Predicted  $^{20}\text{Ne}$ ,  $^{36}\text{Ar}$ ,  $^{84}\text{Kr}$ , and  $^{132}\text{Xe}$  concentrations in the water phase are also calculated for two scenarios: (1) addition of excess air (EA) (green solid lines) and (2) residual water phase following water–gas interaction in a closed-system (red dashed lines) at 18 and 25 °C.

$^4\text{He}$  and  $^4\text{He}^*$  are very similar and point to a dominantly crustal  $^4\text{He}$  component in most samples, as opposed to atmospheric and mantle-derived components (cf. SI Text S3).

Measured R/Ra values vary from an almost pure crustal value of  $0.030 \pm 0.001$  (typical crustal production values are  $\sim 0.02\text{--}0.05$ )<sup>24</sup> for most samples to  $0.889 \pm 0.008$  in a few samples, a value very close to that of the atmosphere. Most of the measured higher R/Ra ratios reflect the impact of mixing between older groundwater and recharge water carrying a pure atmospheric component (R/Ra = 1).<sup>21,47</sup> Our helium component analysis (cf. SI Text S3) also points to the likely presence of a minor but non-negligible mantle He component of up to 2% in some samples (e.g., samples 253 and 364),

which contributes, to a lesser extent, to increased R/Ra values. Irrespective of the presence of an atmospheric or mantle origin for He leading to slightly higher R/Ra values, a  $^4\text{He}^*$  component is largely dominant for most samples. As expected, R/Ra values display an inverse correlation with methane concentrations. This points to increased amounts of  $^4\text{He}^*$  (lower R/Ra values) with increasing methane concentrations thus, strongly suggesting a common source for both methane and  $^4\text{He}^*$  (Figures 2b, c).

Most measured  $^{20}\text{Ne}/^{22}\text{Ne}$  ratios are close to the atmospheric value of 9.80 (SI Table S3).  $^{21}\text{Ne}/^{22}\text{Ne}$  ratios range from  $0.0289 \pm 0.0001$  to  $0.0304 \pm 0.0003$  reflecting the addition of minor but non-negligible crustally produced  $^{21}\text{Ne}^*$

through the nuclear reactions  $^{18}\text{O}(\alpha, n)^{21}\text{Ne}$  and  $^{24}\text{Mg}(n, \alpha)^{21}\text{Ne}$ .<sup>48</sup>  $^{21}\text{Ne}^*$  values are estimated following Ballentine et al.<sup>20</sup> and vary between 0% and 4.8% of total measured  $^{21}\text{Ne}$  with an atmospheric  $^{21}\text{Ne}$  contribution varying between 95.2% and 100%. It is apparent that, for all samples displaying  $^{21}\text{Ne}/^{22}\text{Ne}$  ratios higher than ASW values, a direct correlation between  $^{21}\text{Ne}^*$  and dissolved methane in groundwater is also observed, pointing again to a common origin between crustally produced  $^{21}\text{Ne}^*$  and stray gas present in the Trinity Aquifer (Figure 2d).

All  $^{38}\text{Ar}/^{36}\text{Ar}$  ratios are close to the atmospheric value of 0.188 (SI Table S3). In contrast, some groundwater samples display  $^{40}\text{Ar}/^{36}\text{Ar}$  ratios (samples 355, 358, 369, 533, and 555) above the atmospheric value of 295.5, reflecting the addition of crustally produced  $^{40}\text{Ar}^*$  (SI Table S3; Figure 2e). Similar to excess  $^4\text{He}$  from U and Th, excesses of  $^{40}\text{Ar}$  are commonly observed in old crustal fluids due to the natural decay of  $^{40}\text{K}$  in rock formations.<sup>20,49,50</sup> Contribution of crustally produced  $^{40}\text{Ar}^*$  is estimated following Ballentine et al.<sup>20</sup>  $^{40}\text{Ar}^*$  varies from 0% to 4.6%, with atmospheric  $^{40}\text{Ar}$  varying between 95.4% and 100%. Similar to  $^4\text{He}^*$  and  $^{21}\text{Ne}^*$ ,  $^{40}\text{Ar}^*$  correlates well with dissolved methane concentrations (Figure 2e), pointing once again to an origin similar to that of dissolved methane.

In contrast, all Kr isotopic ratios (e.g.,  $^{86}\text{Kr}/^{84}\text{Kr}$ ) are indistinguishable from the atmospheric values (SI Table S3). Unlike Kr, some groundwater samples display  $^{136}\text{Xe}/^{130}\text{Xe}$  ratios above the atmospheric ratio of 2.176, up to  $2.206 \pm 0.004$ , and point to the presence of excess  $^{136}\text{Xe}$  in these samples (e.g., sample 211B; SI Table S3; Figure 2f). These elevated Xe isotopic ratios suggest the presence of crustal and/or mantle Xe components derived from  $^{238}\text{U}$  spontaneous fission,<sup>51</sup> in addition to the atmospheric component. Unlike R/Ra,  $^{21}\text{Ne}/^{22}\text{Ne}$  and  $^{40}\text{Ar}/^{36}\text{Ar}$  ratios though,  $^{136}\text{Xe}/^{130}\text{Xe}$  ratios display no correlation with dissolved methane concentrations. In contrast to total  $^4\text{He}$ ,  $^{21}\text{Ne}$  and  $^{40}\text{Ar}$ , sedimentary Xe can be released from organic matter that has accumulated Xe due to a diffusion-controlled fractionation process and this may contribute to the total  $^{136}\text{Xe}$ . This contribution may dilute excess  $^{136}\text{Xe}$  and thus weaken the correlation between  $^{136}\text{Xe}/^{130}\text{Xe}$  and methane contents. This hypothesis was previously suggested in the literature.<sup>27,52–55</sup>

**Stray Gas Source and Migration Mechanisms – Production Wells versus Water Wells.** As shown above, dissolved methane concentrations display positive correlations with multiple crustal noble gas isotopes, in particular,  $^4\text{He}^*$ ,  $^{21}\text{Ne}^*$  and  $^{40}\text{Ar}^*$  suggesting that noble gases and methane in the Trinity Aquifer originate from a common source. Here, through a combined analysis of atmospheric-derived  $^{20}\text{Ne}$ ,  $^{36}\text{Ar}$ ,  $^{84}\text{Kr}$  and  $^{132}\text{Xe}$  together with information provided by well logs, we place constraints on the specific stray gas source and, in particular, whether the presence of methane in the Trinity Aquifer might originate from production wells or not have a connection with gas production.

To determine whether this external origin is the Strawn Group or the Barnett Shale and, more importantly, to assess whether or not the presence of stray gas results from a conventional or HF production well, we examine measured  $^{20}\text{Ne}$ ,  $^{36}\text{Ar}$ ,  $^{84}\text{Kr}$ , and  $^{132}\text{Xe}$  concentrations of Trinity Aquifer samples (Figure 3). All four isotopes in these groundwater samples are almost entirely of atmospheric origin and are introduced by freshwater recharge previously equilibrated with the atmosphere (ASW). Predicted ASW  $^{20}\text{Ne}$ ,  $^{36}\text{Ar}$ ,  $^{84}\text{Kr}$ , and

$^{132}\text{Xe}$  concentrations for temperatures varying between 0 and 25 °C are shown (Figures 3a, b, c; bold red line). All groundwater samples from both the south (closed black circles) and north (closed blue squares) clusters are shown. Figure 3a shows that  $^{20}\text{Ne}$  concentrations in most groundwater samples are above the predicted ASW composition. These include all north cluster and most south cluster samples. Because  $^{20}\text{Ne}/^{22}\text{Ne}$  ratios for most samples display atmospheric values within a 2-sigma error and because most samples fall on the predicted excess air-line (cf. Figure 3), most of the observed  $^{20}\text{Ne}$  excesses in these groundwaters are expected to result from incorporation of excess air (EA) due to rapid fluctuations of the water table level.<sup>56</sup> Some previous studies have associated the presence of  $^{20}\text{Ne}$  to an exogenous source, possibly due to natural brine migration. This was the case, for example, of groundwaters within the Marcellus Shale footprint and groundwaters of the Michigan Basin.<sup>8,17,52,57</sup> However, as indicated below, this does not seem to be the case in this study. Significant levels of EA are commonly present in modern Texas groundwaters (e.g., Castro et al.<sup>58</sup>). Predicted  $^{20}\text{Ne}$  and  $^{36}\text{Ar}$  ASW values in water with addition of increasing EA amounts are shown for temperatures of 18 and 25 °C, which correspond to the average mean annual air temperature (MAAT) for Springtown (1962–1978), Weatherford (1946–2014) and Mineral Wells (1948–2014) in north-central Texas (<http://www.ncdc.noaa.gov/cdo-web/search>) and to the highest measured water temperature of Trinity Aquifer groundwater samples,<sup>35</sup> respectively (green solid lines, Figure 3a). In contrast to most samples and as also previously documented by Darrah et al.<sup>8</sup> in a few water wells, four groundwater samples, all from the south cluster (samples 355, 358, 369, and 555; Figure 3a) display  $^{20}\text{Ne}$  and  $^{36}\text{Ar}$  concentrations below the ASW composition and point thus to significant depletion of atmospheric-derived  $^{20}\text{Ne}$  and  $^{36}\text{Ar}$ , that is, stripping of atmospheric noble gases. All four of these groundwater samples have high measured methane concentrations, between ~12 mg/L and ~23 mg/L. In particular, during sampling collection, a sustained natural gas flow of ~3L/min was measured at well 555 (drilled as a water well but not used and left unplugged). The presence of a gas phase (mostly  $\text{CH}_4$ ) within the aquifer in these four groundwater samples leads to exsolution of noble gases. This exsolution will be more severe for the light noble gases and that of  $^{20}\text{Ne}$  in particular, as opposed to the heavier ones ( $^{84}\text{Kr}$  and  $^{132}\text{Xe}$ ) as the lighter noble gases will go preferentially into the gas phase.<sup>59,60</sup> Expected noble gas concentrations in a residual water phase in contact with a gas phase for an initial ASW composition at 18 and 25 °C assuming a closed-system (cf. Ballentine et al.<sup>61</sup>) are shown in Figure 3a (red dashed lines). It is apparent that all these four samples are consistent with predicted stripped water values, sample 555 displaying the most severe depletion with values down to 0.18 and 0.22 times that of ASW at 18 °C for  $^{20}\text{Ne}$  and  $^{36}\text{Ar}$ , respectively (SI Table S2). Similar depletion trends, also consistent with stripping due to the presence of a gas phase, are observed for  $^{84}\text{Kr}$  and  $^{132}\text{Xe}$  (Figures 3b, c) with values down to 0.28 and 0.36 times that of ASW at 18 °C for sample 555, respectively. As expected, the heavier noble gases  $^{84}\text{Kr}$  and  $^{132}\text{Xe}$  point to a lower level of stripping with respect to the lighter noble gases (Figures 3a, b, c). This is clearly observed in sample 533, also with a high methane concentration, where stripping is observed for  $^{20}\text{Ne}$  but not for  $^{36}\text{Ar}$ ,  $^{84}\text{Kr}$  and  $^{132}\text{Xe}$ . These observations likely suggest not only the presence of

localized gas sources but also a short contact time between the gas and liquid phases precluding equilibration between these two phases for the heavier noble gases in well 533. From Figure 3b, c, it is also apparent that sample 533 displays relative enrichment in water-phase atmospheric  $^{132}\text{Xe}$  as opposed to  $^{36}\text{Ar}$  and  $^{84}\text{Kr}$ , which points to an equilibration temperature lower than the MAAT, at around 14 °C (see also, e.g., Castro et al.<sup>58</sup>). This, however, is unrelated to water–gas phase interaction processes.

If a gas phase (gaseous methane) were present throughout the Trinity Aquifer, fractionation of atmospheric noble gas components in the water would be widely observed.<sup>61,62</sup> Because, as pointed out earlier, EA has a greater impact on the light noble gas composition compared to the heavy noble gases (Figures 3a, b, c) in groundwater, we now focus solely on the heavy  $^{84}\text{Kr}$  and  $^{132}\text{Xe}$  noble gases fractionation in an attempt to reduce the impact of EA as much as possible and thus, any potential bias that might result. Unlike  $^{20}\text{Ne}$ , most samples display  $^{84}\text{Kr}$  and  $^{132}\text{Xe}$  corresponding to that of ASW composition as the heavier noble gases are not significantly affected by the EA component.

Figure 4 shows  $F(^{132}\text{Xe}/^{36}\text{Ar})$  versus  $F(^{84}\text{Kr}/^{36}\text{Ar})$  for all collected water samples.  $F(^{132}\text{Xe}/^{36}\text{Ar})$  and  $F(^{84}\text{Kr}/^{36}\text{Ar})$  are

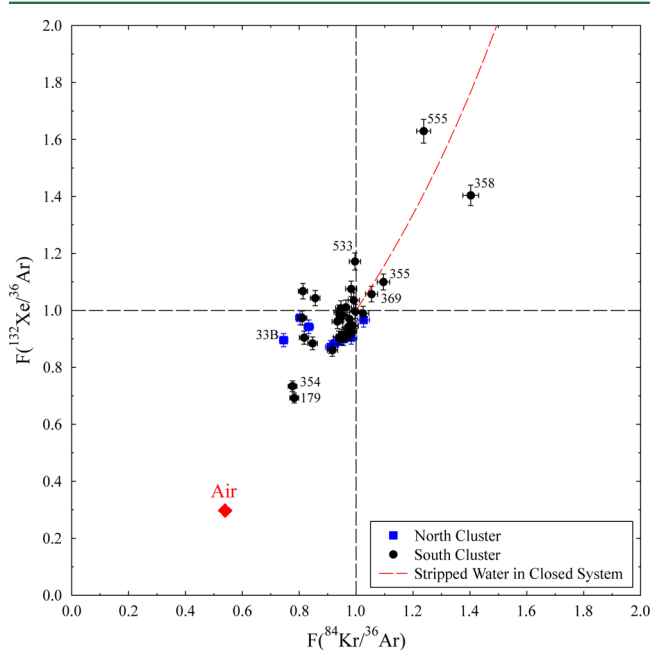


**Figure 4.** Comparison of fractionation  $F$  levels of atmospheric noble gas isotopic ratios  $^{132}\text{Xe}/^{36}\text{Ar}$  versus  $^{84}\text{Kr}/^{36}\text{Ar}$  for all Trinity Aquifer groundwater samples.  $^{132}\text{Xe}/^{36}\text{Ar}$  and  $^{84}\text{Kr}/^{36}\text{Ar}$  ratios are normalized to the ASW value at 18 °C (SI Table S5). The air value is indicated by a red diamond. Calculated closed-system fractionation curve (red dashed line; cf. Ballentine et al.<sup>61</sup>) for a residual water phase that has an initial ASW composition at 18 °C is also shown.

measured ratios normalized to corresponding ASW values at 18 °C (MAAT) of  $2.51 \times 10^{-3}$  and  $3.83 \times 10^{-2}$  for  $^{132}\text{Xe}/^{36}\text{Ar}$  and  $^{84}\text{Kr}/^{36}\text{Ar}$ , respectively (SI Table S5 and Figure S7). The air value (red diamond) as well as the calculated closed system fractionation curve (red dashed line; cf. Ballentine et al.<sup>61</sup>) for a residual water phase that has an initial ASW composition at 18 °C are also shown. From Figure 4, it is apparent that most water samples display minimal fractionation in  $^{132}\text{Xe}/^{36}\text{Ar}$  and  $^{84}\text{Kr}/^{36}\text{Ar}$  ratios. In contrast, those samples with the highest

methane contents do show significant fractionation. Samples 555 and 358 with the highest methane concentrations show, by far, the greatest fractionation, with  $F(^{132}\text{Xe}/^{36}\text{Ar})$  and  $F(^{84}\text{Kr}/^{36}\text{Ar})$  of 1.629 and 1.403, respectively (see also SI Figure S7). In contrast, samples 355 and 369, which also have elevated methane concentrations show only minor fractionation. The observed fractionation in these four samples which, as discussed above, underwent stripping of all atmospheric noble gases (Figures 3a–c) is consistent with water–gas phase interactions in a closed-system model. It should be noted that large quantities of EA in samples 179 and 354 drive their  $F(^{132}\text{Xe}/^{36}\text{Ar})$  and  $F(^{84}\text{Kr}/^{36}\text{Ar})$  values closer to that of air. The fact that only four samples (i.e., 355, 358, 369, and 555) show visible fractionation for all noble gases points, as suggested earlier, to localized gas-phase methane sources in the vicinity of these four wells, indicating that other water samples have likely never been in contact with a gas phase. If that were the case, significant stripping and fractionation of noble gases should be visible in dissolved noble gases in the Trinity Aquifer groundwater with  $F$  values following either a closed or open system fractionation curves (that is, in the upper right quadrant). Thanks to a downhole camera, we observed a continuous source of natural gas actively migrating into well 555 since well completion in 2012, a confirmation that water exposed to a natural gas pocket will show heavy noble gas depletion. Additional information on natural gas accumulations in the Strawn is provided in SI Text S4. Several hydrocarbon fields hosted in the Strawn Group are present in Parker and Hood counties.<sup>63</sup>

A close analysis of driller log data available for these wells shows that all four of these wells are drilled through the unconformity into the Strawn Group as opposed to being only in the Trinity Group. It is likely that shallow noncommercial small gas accumulations, as are known to exist in the Strawn, were reached by these water wells (e.g., well 555) or that the wellbores are located close to one (e.g., well 358). Heavy depletion of atmospheric noble gases and, in particular, of the heavier  $^{84}\text{Kr}$  and  $^{132}\text{Xe}$  in only these four wells is consistent with continuously sustained gas-phase methane migration from a nearby source. Comparison of noble gas analyses from this stray gas and that from the Barnett Shale and Strawn Group further reinforce the finding that the source of the gas is in the Strawn Group (see also Nicot et al.<sup>35</sup>). Darrah et al.<sup>8</sup> and Kornacki and McCaffrey<sup>9</sup> have also concluded that the source of stray gas in these groundwater samples is likely the Strawn Group as opposed to the Barnett Shale.

In contrast to these four water wells with high dissolved methane concentrations showing depleted  $^{20}\text{Ne}$ ,  $^{36}\text{Ar}$ ,  $^{84}\text{Kr}$ , and  $^{132}\text{Xe}$ , other water wells with significantly lower methane concentrations that display expected or higher than ASW  $^{20}\text{Ne}$ ,  $^{36}\text{Ar}$ ,  $^{84}\text{Kr}$ , and  $^{132}\text{Xe}$  concentrations have also penetrated the Strawn Group and do not show stripping of heavy noble gases. The discrete distribution of small shallow natural gas accumulations in the Strawn explains both the scattered distribution of water wells with high methane concentrations and noble gas stripping as well as the presence of water wells penetrating into the Strawn Group but displaying significantly lower methane concentrations.

SI Figures S8a, c, e show  $F(^{132}\text{Xe}/^{36}\text{Ar})$  as a function of distance to the nearest production well (Barnett and/or non-Barnett well) for all collected water samples. From SI Figures S8a, c, e, it is apparent that  $F(^{132}\text{Xe}/^{36}\text{Ar})$  in water samples is not correlated with distance to nearest Barnett gas well ( $r =$

0.19;  $P = 0.20$ ), distance to nearest non-Barnett gas well ( $r = 0.01$ ;  $P = 0.95$ ) and distance to nearest gas production well ( $r = 0.02$ ;  $P = 0.91$ ; including both Barnett and non-Barnett). This lack of correlation further reinforces the hypothesis that dissolved gas in wells with high methane content has a natural origin and likely migrates into the Trinity Aquifer from the Strawn Group through natural pathways such as Strawn sandstone lenses in hydrological contact with Trinity Sands as opposed to faulty production wells as previously suggested.<sup>8</sup>

By comparing  $^4\text{He}/^{20}\text{Ne}$  ratios of dissolved gas in groundwater samples and of natural gases from the Strawn Group, the impact of gas production wells can be evaluated.<sup>8</sup> With Strawn gas migrating away from production wells (Barnett and/or non-Barnett wells),  $^4\text{He}/^{20}\text{Ne}$  values in groundwater should display a gradual decrease from the  $^4\text{He}/^{20}\text{Ne}$  values observed in Strawn natural gases<sup>8</sup> (4800–29 000; gray domain in SI Figures S8b, d, f) to the ASW value at MAAT (0.265; dashed line in SI Figures S8b, d, f). However,  $^4\text{He}/^{20}\text{Ne}$  values show a complete absence of correlation with distance to nearest Barnett gas well ( $r = 0.20$ ;  $P = 0.19$ ), distance to nearest non-Barnett gas well ( $r = 0.09$ ;  $P = 0.55$ ) and distance to nearest gas production well ( $r = 0.07$ ;  $P = 0.66$ ; including both Barnett and non-Barnett), and thus do not support the notion that stray gas present in these water wells migrated from some nearby production wells from leaks along faulty surface casing as suggested by previous research.<sup>8</sup>

Furthermore, positive correlation between  $\text{CH}_4/^{36}\text{Ar}$  ratios and  $\text{Cl}^-$  concentrations in water would indicate natural or anthropogenic deep brine migration.<sup>8</sup> However, no correlation between  $\text{CH}_4/^{36}\text{Ar}$  with  $\text{Cl}^-$  is observed for samples either above or below the  $\text{CH}_4$  saturation line ( $r = 0.12$ ;  $P = 0.48$ ; SI Figure S9). Therefore, based on  $\text{CH}_4/^{36}\text{Ar}$  ratio versus  $\text{Cl}^-$  concentrations in water and/or on calculated  $^4\text{He}/^{20}\text{Ne}$  values, there is no basis at this stage to infer an influx of deep brine along with stray gas either from leaks of production wells or from natural flow along minor faults. Rather, our findings suggest that stray gas in the Trinity Aquifer is likely related to noncommercial small gas accumulations in the Strawn Group. At this stage, none of our observations and measurements points to migration of stray gas from nearby Strawn or Barnett production wells.

## ■ ASSOCIATED CONTENT

### ● Supporting Information

The Supporting Information is available free of charge on the ACS Publications website at DOI: 10.1021/acs.est.6b01494.

Supporting Texts S1 to S4 and Figures S1 to S9 and Tables S1 to S5 (PDF)

## ■ AUTHOR INFORMATION

### Corresponding Author

\*Phone: (734) 615-3812; fax: (734) 763-4690; e-mail: mccastro@umich.edu.

### Notes

The authors declare no competing financial interest.

## ■ ACKNOWLEDGMENTS

Funding for this project was provided by RPSEA award 11122-56 through the "Ultra-Deepwater and Unconventional Natural Gas and Other Petroleum Resources" program authorized by the U.S. Energy Policy Act of 2005. NSF grant EAR #1049822 provided additional financial support. We thank the editor as

well as two reviewers for their insightful and thorough reviews. We also thank all well owners for access to their water wells as well as Laura Bouvier for her assistance in the field and IHS for free access to their Enerdeq database.

## ■ REFERENCES

- (1) Nicot, J.-P.; Scanlon, B. R.; Reedy, R. C.; Costley, R. A. Source and Fate of Hydraulic Fracturing Water in the Barnett Shale: A Historical Perspective. *Environ. Sci. Technol.* **2014**, *48* (4), 2464–2471.
- (2) Nicot, J.-P.; Scanlon, B. R. Water Use for Shale-Gas Production in Texas, U.S. *Environ. Sci. Technol.* **2012**, *46* (6), 3580–3586.
- (3) USEIA *Annual Energy Outlook 2015*; US Energy Information Administration: Washington, DC, 2015.
- (4) Jackson, R. B.; Vengosh, A.; Darrah, T. H.; Warner, N. R.; Down, A.; Poreda, R. J.; Osborn, S. G.; Zhao, K.; Karr, J. D. Increased stray gas abundance in a subset of drinking water wells near Marcellus shale gas extraction. *Proc. Natl. Acad. Sci. U. S. A.* **2013**, *110* (28), 11250–11255.
- (5) Molofsky, L. J.; Connor, J. A.; Wylie, A. S.; Wagner, T.; Farhat, S. K. Evaluation of Methane Sources in Groundwater in Northeastern Pennsylvania. *Groundwater* **2013**, *51* (3), 333–349.
- (6) Osborn, S. G.; Vengosh, A.; Warner, N. R.; Jackson, R. B. Methane contamination of drinking water accompanying gas-well drilling and hydraulic fracturing. *Proc. Natl. Acad. Sci. U. S. A.* **2011**, *108* (20), 8172–8176.
- (7) Thompson, H. Fracking boom spurs environmental audit. *Nature* **2012**, *485* (7400), 556–557.
- (8) Darrah, T. H.; Vengosh, A.; Jackson, R. B.; Warner, N. R.; Poreda, R. J. Noble gases identify the mechanisms of fugitive gas contamination in drinking-water wells overlying the Marcellus and Barnett Shales. *Proc. Natl. Acad. Sci. U. S. A.* **2014**, *111* (39), 14076–14081.
- (9) Kornacki, A. S.; McCaffrey, M. Monitoring the Active Migration and Biodegradation of Natural Gas in the Trinity Group Aquifer at the Silverado Development in Southern Parker County, Texas; *AAPG Annual Convention and Exhibition*. April 7, 2014.
- (10) Moritz, A.; Helie, J.-F.; Pinti, D. L.; Larocque, M.; Barnette, D.; Retailliau, S.; Lefebvre, R.; Gelin, Y. Methane Baseline Concentrations and Sources in Shallow Aquifers from the Shale Gas-Prone Region of the St. Lawrence Lowlands (Quebec, Canada). *Environ. Sci. Technol.* **2015**, *49* (7), 4765–4771.
- (11) Li, H.; Carlson, K. H. Distribution and Origin of Groundwater Methane in the Wattenberg Oil and Gas Field of Northern Colorado. *Environ. Sci. Technol.* **2014**, *48* (3), 1484–1491.
- (12) Siegel, D.; Smith, B.; Perry, E.; Bothun, R.; Hollingsworth, M. Dissolved methane in shallow groundwater of the Appalachian Basin: Results from the Chesapeake Energy predrilling geochemical database. *Environ. Geosci.* **2016**, *23* (1), 1–47.
- (13) Siegel, D. I.; Azzolina, N. A.; Smith, B. J.; Perry, A. E.; Bothun, R. L. Methane Concentrations in Water Wells Unrelated to Proximity to Existing Oil and Gas Wells in Northeastern Pennsylvania. *Environ. Sci. Technol.* **2015**, *49* (7), 4106–4112.
- (14) Lollar, B. S.; Ballentine, C. J. *Nat. Geosci.* **2009**, *2* (8), 543–547.
- (15) Ozima, M.; Podosek, F. A. *Noble Gas Geochemistry*; Cambridge University Press: New York, 2002.
- (16) Hilton, D. R.; Porcelli, D. 2.06 - Noble Gases as Mantle Tracers. In *Treatise on Geochemistry*; Turekian, H. D. H. K., Ed.; Treatise on Geochemistry; Pergamon: Oxford, 2003; pp 277–318.
- (17) Castro, M. C.; Ma, L.; Hall, C. M. A primordial, solar He–Ne signature in crustal fluids of a stable continental region. *Earth Planet. Sci. Lett.* **2009**, *279* (3–4), 174–184.
- (18) Pinti, D. L.; Castro, M. C.; Shouakar-Stash, O.; Tremblay, A.; Garduño, V. H.; Hall, C. M.; Hélie, J. F.; Ghaleb, B. Evolution of the geothermal fluids at Los Azufres, Mexico, as traced by noble gas isotopes,  $\delta^{18}\text{O}$ ,  $\delta\text{D}$ ,  $\delta^{13}\text{C}$  and  $87\text{Sr}/86\text{Sr}$ . *J. Volcanol. Geotherm. Res.* **2012**, *249* (0), 1–11.

- (19) Porcelli, D.; Ballentine, C. J.; Wieler, R. An Overview of Noble Gas Geochemistry and Cosmochemistry. *Rev. Mineral. Geochem.* **2002**, *47* (1), 1–19.
- (20) Ballentine, C. J.; O’niions, R. K.; Oxburgh, E. R.; Horvath, F.; Deak, J. Rare gas constraints on hydrocarbon accumulation, crustal degassing and groundwater flow in the Pannonian Basin. *Earth Planet. Sci. Lett.* **1991**, *105* (1–3), 229–246.
- (21) Castro, M. C.; Jambon, A.; de Marsily, G.; Schlosser, P. Noble gases as natural tracers of water circulation in the Paris Basin: 1. Measurements and discussion of their origin and mechanisms of vertical transport in the basin. *Water Resour. Res.* **1998**, *34* (10), 2443–2466.
- (22) Castro, M. C.; Goblet, P.; Ledoux, E.; Violette, S.; de Marsily, G. Noble gases as natural tracers of water circulation in the Paris Basin: 2. Calibration of a groundwater flow model using noble gas isotope data. *Water Resour. Res.* **1998**, *34* (10), 2467–2483.
- (23) Kulongoski, J. T.; Hilton, D. R.; Izbicki, J. A. Source and movement of helium in the eastern Morongo groundwater Basin: The influence of regional tectonics on crustal and mantle helium fluxes. *Geochim. Cosmochim. Acta* **2005**, *69* (15), 3857–3872.
- (24) Oxburgh, E. R.; O’niions, R. K.; Hill, R. I. Helium isotopes in sedimentary basins. *Nature* **1986**, *324* (6098), 632–635.
- (25) Pinti, D. L.; Marty, B. Noble gases in crude oils from the Paris Basin, France: Implications for the origin of fluids and constraints on oil-water-gas interactions. *Geochim. Cosmochim. Acta* **1995**, *59* (16), 3389–3404.
- (26) Warriar, R. B.; Castro, M. C.; Hall, C. M.; Lohmann, K. C. Large atmospheric noble gas excesses in a shallow aquifer in the Michigan Basin as indicators of a past mantle thermal event. *Earth Planet. Sci. Lett.* **2013**, *375* (0), 372–382.
- (27) Wen, T.; Castro, M. C.; Ellis, B. R.; Hall, C. M.; Lohmann, K. C. Assessing compositional variability and migration of natural gas in the Antrim Shale in the Michigan Basin using noble gas geochemistry. *Chem. Geol.* **2015**, *417*, 356–370.
- (28) Wen, T.; Castro, M. C.; Hall, C. M.; Pinti, D. L.; Lohmann, K. C. Constraining groundwater flow in the glacial drift and saginaw aquifers in the Michigan Basin through helium concentrations and isotopic ratios. *Geofluids* **2016**, *16*, 3–25.
- (29) Holland, G.; Gilfillan, S. Application of noble gases to the viability of CO<sub>2</sub> storage. In *The Noble Gases as Geochemical Tracers*; Burnard, P., Ed.; Springer: Berlin, 2013; pp 177–223.
- (30) Pollastro, R. M.; Jarvie, D. M.; Hill, R. J.; Adams, C. W. Geologic framework of the Mississippian Barnett Shale, Barnett-Paleozoic total petroleum system, Bend arch–Fort Worth Basin, Texas. *AAPG Bull.* **2007**, *91* (4), 405–436.
- (31) Montgomery, S. L.; Jarvie, D. M.; Bowker, K. A.; Pollastro, R. M. Mississippian Barnett Shale, Fort Worth basin, north-central Texas: Gas-shale play with multi–trillion cubic foot potential. *AAPG Bull.* **2005**, *89* (2), 155–175.
- (32) Hill, R. J.; Jarvie, D. M.; Zumberge, J.; Henry, M.; Pollastro, R. M. Oil and gas geochemistry and petroleum systems of the Fort Worth Basin. *AAPG Bull.* **2007**, *91* (4), 445–473.
- (33) Nicot, J. P.; Huang, Y.; Wolaver, B. D.; Costley, R. A. Flow and salinity patterns in the low-transmissivity Upper Paleozoic aquifers of North-Central Texas. *GCAGS Journal* **2013**, *2*, 53–67.
- (34) Bruner, K. R.; Smosna, R. *A comparative study of the Mississippian Barnett Shale, Fort Worth Basin, and Devonian Marcellus Shale*; DOE/NETL, 2011.
- (35) Nicot, J.-P.; Mickler, P.; Larson, T.; Castro, M. C.; Darvari, R.; Smyth, R.; Uhman, K.; Omelon, C. *Understanding and Managing Environmental Roadblocks to Shale Gas Development: An Analysis of Shallow Gas, NORM, and Trace Metals*; Research Partnership to Secure Energy for America: Austin, 2015; <http://www.rpsea.org/projects/11122-56/>.
- (36) Herkommer, M. A.; Denke, G. W. *Stratigraphy and Hydrocarbons*; Dallas Geological Society: Parker County, TX, 1982.
- (37) Hackley, P. C.; Guevara, E. H.; Hentz, T. F.; Hook, R. W. Thermal maturity and organic composition of Pennsylvanian coals and carbonaceous shales, north-central Texas: Implications for coalbed gas potential. *Int. J. Coal Geol.* **2009**, *77* (3–4), 294–309.
- (38) Kreitler, C. W. *Lessons Learned from the Barnett Shale Range Resources Litigation*; Hydraulic Fracturing and Environmental Implications: Austin, 2014; pp 1–75.
- (39) Henry, J. D. Stratigraphy of the Barnett Shale (Mississippian) and Associated Reefs in the Northern Fort Worth Basin. *Petroleum Geology of the Fort Worth Basin and Bend Arch Area* **1982**, 157–177.
- (40) Van, A.; Kelley, Ewing, J.; Jones, T. L.; Young, S. C.; Deeds, N.; Hamlin, S. *Updated Groundwater Availability Model of the Northern Trinity and Woodbine Aquifers*; Texas Water Development Board, 2014; pp 1–990.
- (41) Ewing, T. E. *The tectonic framework of Texas: Text accompanying the tectonic map of Texas*; Texas Bureau of Economic Geology, 1991.
- (42) Weiss, R. F. Piggyback sampler for dissolved gas studies on sealed water samples. *Deep-Sea Res. Oceanogr. Abstr.* **1968**, *15* (6), 695–699.
- (43) Kampbell, D. H.; Vandegriff, S. A. Analysis of dissolved methane, ethane, and ethylene in ground water by a standard gas chromatographic technique. *J. Chromatogr. Sci.* **1998**, *36* (5), 253–256.
- (44) Eltschlager, K. K.; Hawkins, J. W.; Ehler, W. C.; Baldassare, F. *Technical Measures for the Investigation and Mitigation of Fugitive Methane Hazards in Areas of Coal Mining*; Department of the Interior Office of Surface Mining, 2001.
- (45) Clarke, W. B.; Jenkins, W. J.; Top, Z. Determination of tritium by mass spectrometric measurement of <sup>3</sup>He. *Int. J. Appl. Radiat. Isot.* **1976**, *27* (9), 515–522.
- (46) Castro, M. C.; Stute, M.; Schlosser, P. Comparison of <sup>4</sup>He ages and <sup>14</sup>C ages in simple aquifer systems: implications for groundwater flow and chronologies. *Appl. Geochem.* **2000**, *15* (8), 1137–1167.
- (47) Castro, M. C. Helium sources in passive margin aquifers—new evidence for a significant mantle <sup>3</sup>He source in aquifers with unexpectedly low in situ <sup>3</sup>He/<sup>4</sup>He production. *Earth Planet. Sci. Lett.* **2004**, *222* (3), 897–913.
- (48) Wetherill, G. Variations in the Isotopic Abundances of Neon and Argon Extracted from Radioactive Minerals. *Phys. Rev.* **1954**, *96* (3), 679–683.
- (49) Ballentine, C. J.; Mazurek, M.; Gautschi, A. Thermal constraints on crustal rare gas release and migration: Evidence from Alpine fluid inclusions. *Geochim. Cosmochim. Acta* **1994**, *58* (20), 4333–4348.
- (50) Ma, L.; Castro, M. C.; Hall, C. M. Crustal noble gases in deep brines as natural tracers of vertical transport processes in the Michigan Basin. *Geochem., Geophys., Geosyst.* **2009**, *10* (6), Q06001.
- (51) Eikenberg, J.; Signer, P.; Wieler, R. U-Xe, U-Kr, and U-Pb systematics for dating uranium minerals and investigations of the production of nucleogenic neon and argon. *Geochim. Cosmochim. Acta* **1993**, *57* (5), 1053–1069.
- (52) Ma, L.; Castro, M. C.; Hall, C. M. Atmospheric noble gas signatures in deep Michigan Basin brines as indicators of a past thermal event. *Earth Planet. Sci. Lett.* **2009**, *277* (1–2), 137–147.
- (53) Podosek, F. A.; Honda, M.; Ozima, M. Sedimentary noble gases. *Geochim. Cosmochim. Acta* **1980**, *44* (11), 1875–1884.
- (54) Torgersen, T.; Kennedy, B. M. Air-Xe enrichments in Elk Hills oil field gases: role of water in migration and storage. *Earth Planet. Sci. Lett.* **1999**, *167* (3–4), 239–253.
- (55) Zhou, Z.; Ballentine, C. J.; Kipfer, R.; Schoell, M.; Thibodeaux, S. Noble gas tracing of groundwater/coalbed methane interaction in the San Juan Basin, USA. *Geochim. Cosmochim. Acta* **2005**, *69* (23), 5413–5428.
- (56) Heaton, T. H. E.; Vogel, J. C. Excess air” in groundwater. *J. Hydrol.* **1981**, *50* (0), 201–216.
- (57) Darrach, T. H.; Jackson, R. B.; Vengosh, A.; Warner, N. R.; Whyte, C. J.; Walsh, T. B.; Kondash, A. J.; Poreda, R. J. The evolution of Devonian hydrocarbon gases in shallow aquifers of the northern Appalachian Basin: Insights from integrating noble gas and hydrocarbon geochemistry. *Geochim. Cosmochim. Acta* **2015**, *170*, 321–355.
- (58) Castro, M. C.; Hall, C. M.; Patriarche, D.; Goblet, P.; Ellis, B. R. A new noble gas paleoclimate record in Texas — Basic assumptions revisited. *Earth Planet. Sci. Lett.* **2007**, *257* (1–2), 170–187.

(59) Bosch, A.; Mazor, E. Natural gas association with water and oil as depicted by atmospheric noble gases: case studies from the southeastern Mediterranean Coastal Plain. *Earth Planet. Sci. Lett.* **1988**, *87* (3), 338–346.

(60) Zartman, R. E.; Wasserburg, G. J.; Reynolds, J. H. Helium, argon, and carbon in some natural gases. *J. Geophys. Res.* **1961**, *66* (1), 277–306.

(61) Ballentine, C. J.; Burgess, R.; Marty, B. Tracing Fluid Origin, Transport and Interaction in the Crust. *Rev. Mineral. Geochem.* **2002**, *47* (1), 539–614.

(62) Pinti, D. L.; Marty, B. Chapter 7. Noble Gases in Oil and Gas Fields: Origins and Processes; Fluids and Basin Evolution. *Mineral Soc. Can. Short Course* **2000**, *28*, 160–196.

(63) Ehlmann, A. J.; Ehlmann, R. J. the Aledo Southeast (1200' Strawn) Gas Field and Associated Deeper Production, Southeast Parker and Southwest Tarrant Counties, Texas; *AAPG Southwest Section*, 1985.